Aalborg Universitet

Enabling Real-Time Impedance Measurements of Operational Superconducting Circuits of Accelerator Magnets

Christensen, Magnus Bøg Borregaard; Bednarek, Mateusz; Denz, Reiner; Koch, Peter; Ludwin, Jaromir; Rodriguez-Mateos, Felix; Podzorny, Tomasz; Ravaioli, Emmanuele; Steckert, Jens; Verweij, Arjan; Wozniak, Mariusz; Østergaard, Jan

[Link to publication from Aalborg University](#)

Enabling Real-Time Impedance Measurements of Operational Superconducting Circuits of Accelerator Magnets

M. B. B. Christensen [1,2], M. J. Bednarek [1], R. Denz [1], P. Koch [2], J. Ludwin [1,3], F. Rodriguez-Mateos[1], T. Podzorny [1], E. Ravaioli [1], J. Steckert [1], A. Verweij [1], M. Wozniak [1], and J. Østergaard [2]

[1]European Organization for Nuclear Research, Geneva, Switzerland
[2]Aalborg University, Aalborg, Denmark
[3]Institute of Nuclear Physics Polish Academy of Sciences, Krakow, Poland

Abstract—Impedance measurements of superconducting circuits routinely serve as means to anticipate their dynamic response and validate their electrical integrity. Usual procedures involve performing tests on non-powered systems during commissioning and maintenance periods. However, impedance measurements might have a strong potential in diagnostics of powered superconducting circuits as well. In particular, they should allow for on-line fault monitoring, enhanced quench detection, and deeper insight into the electrical properties of the circuits such as impedance variations or non-linear effects in the operational conditions. This paper outlines the design of an experimental platform enabling such an evaluation. In essence, this system is capable of injecting electrical stimuli into a magnet circuit and capturing the response. The acquired data are processed in order to extract circuit characteristics, in particular the impedance and its temporal evolution. In addition to discussing key design considerations related to measurement performance such as bandwidth, resolution, and sensitivity, the paper explores how to maintain transparent operation with respect to peripheral components such as the power converters and quench protection systems. Finally, the paper presents the validation campaign of the designed solution. The validation consists of two stages, including non-powered and powered superconducting circuits. The former case compares performance of the system to a state-of-the-art industrial impedance analyser, while the latter focuses on the impact the system has on peripheral components. Presented conclusions provide guidelines for front-end instrumentation design and data processing in order to enhance performance evaluation of superconducting circuits in their entire operational spectrum.

Index Terms—Accelerator magnets, fault diagnosis, impedance, quench protection, test equipment

I. INTRODUCTION

MODERN particle accelerator facilities rely on superconducting magnets to maximise the energy of an accelerated particle beam. Prior to operation, each magnet undergoes rigorous testing, including measurements of its electrical impedance spectrum as a function of frequency [1]. These impedance spectra are reassessed during subsequent maintenance periods. While the absolute numerical values of the measured impedance spectra may not directly relate to the magnet's operational condition, temporal variations could signal a change in its performance, potentially necessitating more detailed diagnostics. However, due to the infrequent nature of these measurement campaigns, anomalies may go undetected for extended periods, and possibly grow to larger issues with operational impact before being identified. This research proposes a novel approach to continuously capture the impedance spectrum of a magnet circuit in operational conditions. This would allow for diagnostics to be performed with no down time and aid in preemptive maintenance. Given the ability to measure impedances in sufficiently short time intervals, the prospects of such a system extend beyond electrical integrity measurements, and could enable quench detection through instantaneous impedance changes of a magnet circuit.

Hitherto, electrical qualification impedance measurements have been performed using standard industrial impedance analysers. These work by exciting the device under test using a sinusoid at one specified frequency. The current provided by the measuring device and the voltage across the magnet are simultaneously measured. The magnitude ratio and phase difference of these quantities provide the impedance at that particular frequency. To obtain the impedance across a frequency spectrum, this procedure is repeated for a number of frequencies in the frequency window of interest. Although conventional industrial impedance analyzers provide highly accurate impedance measurements, they generally are not suitable for conducting real-time measurements of powered superconducting magnets for three main reasons: First, these devices are typically optimized for stimuli of amplitudes larger than 1 V, which can potentially interfere with power converters, trip safety equipment, or disrupt the particle beam. Second, they are not necessarily designed with the extended input protection required for operating attached to live superconducting circuits. Lastly, they can only measure a single frequency at any given time, limiting their capacity for fast real-time measurements.

This paper presents a system addressing all of the above concerns, thus allowing for continuous impedance spectroscopy of superconducting magnet circuits without affecting the operational performance of peripheral components. Furthermore, strategies for mitigating the inherent trade-off between stringent power and time constraints and the achievable signal-to-noise ratio are explored.
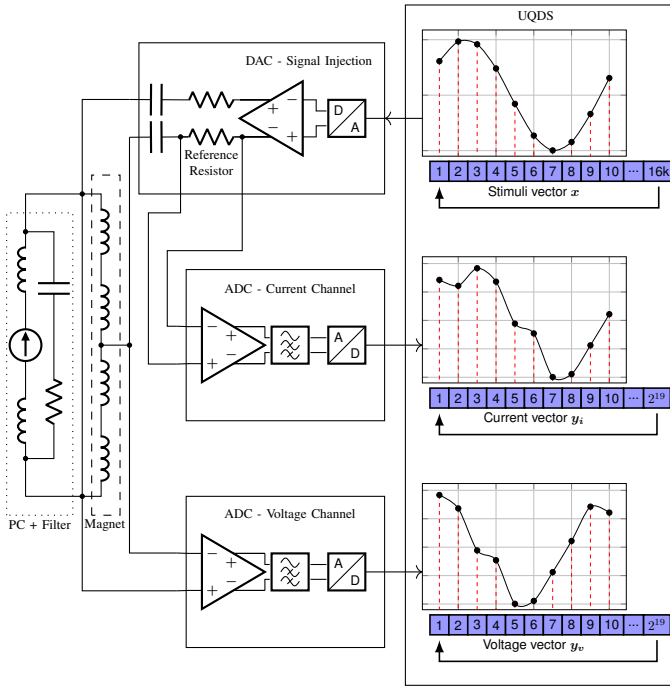
II. METHODOLOGY

A. Hardware

Fig. 1. Block Diagram of the Integrated System. The flow from left to right delineates the major subsystems: a superconducting circuit equipped with a power converter and associated filtering, used for powering the four coils in the MBRD magnet, a DAC Card, employed to inject a signal into the magnet, ADC Cards utilized for measuring voltage and current. These cards interface with the UQDS's FPGA. The EDAQ System facilitates communication between the UQDS and an external PC that can process the data offline (not shown).

Rather than developing a bespoke system, the proposed system's design is built on top of the Universal Quench Detection System (UQDS) developed at CERN [2] [3]. The UQDS is a modular FPGA-based platform supporting large amount of I/O and was designed to interface with up to 32 galvanically isolated ADC channels each sampling at up to $625 \, \text{kS/s}$. The onboard FPGA configures gain and sampling settings of the individual ADC channels. During operation the FPGA synchronously triggers the ADC's and transfers the collected data onto onboard RAM. Depending on configuration, the UQDS can store a total of 2^{19} readings per channel. To configure the UQDS channels and read the collected buffers, CERN's Ethernet Data Acquisition (EDAQ) system is used [4] [5].

For the purpose of this research, the UQDS supports the relevant acquisition capabilities required. However, to perform impedance spectroscopy, it is lacking the capability to inject electrical stimuli into a load. Thus as part of this research the UQDS has been extended to support an AC-coupled 20-bit $500 \, \text{kS/s}$ DAC output stage. In an effort to minimize the operational impact on peripheral systems, the output signal is attenuated. Specifically, the signal should not be able to

inadvertently trip the quench protection attached to the magnet circuit under test. Furthermore, so as to not interfere with the magnet's power-converter's constant current feedback loop, the injected signal power should ideally remain well below the power converter's noise output. The emitted noise varies among the various individual power converter designs, however CERN generally accepts up to $14 \, \text{mV}$ P2P noise for any given $200 \, \text{Hz}$ bandwidth [6]. For the implementation presented in this paper, the attenuation level has been configured to limit the DAC full-scale output range to +/- $16 \, \text{mV}$. If this is not sufficient, additional digital attenuation can be implemented at the cost of reduced resolution.

To allow the injected current to be measured, a reference resistor is placed in series with the output stage. The optimal resistance of this resistor depends on the impedance of the magnet being measured. Since the system is not presently targeted at any specific magnet, a value of $10 \, \Omega \pm 1\%$ is used as it represents the midpoint on a log scale between the 1 and $100 \, \Omega$ commonly being used in impedance analyzers for impedance measurements of superconducting magnets.

To control the output waveform the UQDS FPGA firmware was updated to include a circular buffer supporting up to 16000 predetermined output samples, i.e. a signal of $32 \, \text{ms}$ duration when sampling at the maximum sample rate of $500 \, \text{kS/s}$. The size of this buffer was constrained by the available logic on the UQDS FPGA. A custom waveform is uploaded to the UQDS through the EDAQ interface.

Furthermore, regular UQDS ADC channels are unsuitable for this research. They were specifically designed to detect quenches by sensing the voltage drop developed in the resistive area of a quenched volume, thus requiring them to be sensitive to low-frequency signals [3]. As the proposed use-case demands contrary specification, i.e. high sensitivity to high-frequency signals, a new set of channels with a re-specified signal-conditioning front-end has also been designed as part of this research. These new channels include a high-gain amplifier to maximise the effective resolution in the DAC +/- $16 \, \text{mV}$ output range. Due to this increased sensitivity, high-pass filtering is required to ensure that the channels are not saturated by the power converter noise. For the experiments presented in this paper, 2nd order filtering with a cutoff frequency of $1 \, \text{kHz}$ was used. Like the previous choice of reference resistor and attenuation level, the exact cut-off of this filter is subject to future optimization. A full overview of the hardware chain is shown in Fig. 1.

B. Stimuli Signal Design

To conduct impedance spectroscopy, we must first define an appropriate stimuli signal. Many have been proposed, with multi-sine and pseudorandom binary sequence (PRBS) generally being considered the best [7]. For this paper we focus on multi-sine stimulus, as PRBS requires hardware with higher slew rates than what the currently designed DAC stage allows.

A sampled multisine signal composed of $K \in \mathbb{N}$ sinusoids and $N \in \mathbb{N}$ samples can be represented as [8]:

$$x_n = \sum_{k=1}^{K} b_k \cos\left(\omega_k n + \phi_k\right) \qquad (1)$$

where:

$\boldsymbol{x} \in \mathbb{R}^N$ is the sample vector.

$\boldsymbol{b}, \boldsymbol{\phi}, \boldsymbol{\omega} \in \mathbb{R}^K$ are the amplitude, phase, and sample-rate normalized frequency vectors respectively of the K sinusoids.

In the context of the designed measurement platform, N is the size of the RAM storing the sampled waveform, $\boldsymbol{x}$. However, the size of the circular buffer storing the output waveform, $M \in \mathbb{N}$ must also be considered as it constraints the choice of frequency components. Specifically, $\boldsymbol{x}$ must be periodic in M samples to avoid discontinuities in the output waveform. Thus the individual frequency components, $\boldsymbol{\omega}$, must have periods that are integer multiples of M. With this in mind, $\boldsymbol{\omega}$ is designed to contain a set of up to $L \in \mathbb{N}$ logarithmically spaced frequencies in the range $f_{\min}$ to $f_{\max}$.

$$\boldsymbol{\omega} = \left[\lfloor f_{\min}\rceil, \lfloor f_{\min}10^{\Delta}\rceil, \lfloor f_{\min}10^{2\Delta}\rceil, \ldots, \lfloor f_{\max}\rceil\right]^T \qquad (2)$$

where:

$\boldsymbol{\omega}$ is a vector with unique entries (i.e. any duplicate frequencies that may appear due to rounding are removed) of length K, with $K \leq L$

$f_{\min}/f_{\max}$ is the minimum/maximum normalized frequency

$\Delta = \frac{\log_{10}\frac{f_{\max}}{f_{\min}}}{L-1}$

$\lfloor\rceil$ denotes rounding to the nearest multiple of $\frac{1}{M}$

L is the maximum number of frequencies in $\boldsymbol{\omega}$

Finally, the magnitude, b_k, and phase, ϕ_k, of each frequency must be chosen. The magnitude is set to unity across all frequencies. However, when setting the phases, more care is required to avoid the individual sinusoids interfering to generate a signal with unnecessary high peak-to-average power ratio (PAPR):

$$\text{PAPR} = \frac{\|\boldsymbol{x}\|_\infty^2}{\boldsymbol{x}_{\text{rms}}^2} \quad \text{where } \boldsymbol{x}_{\text{rms}} = \frac{\|\boldsymbol{x}\|_2}{\sqrt{N}}. \qquad (3)$$

Given that we are operating at low voltage levels, it is critical to reduce the PAPR of the stimuli signal to maximise the possible signal-to-noise ratio achievable within the DAC's limited operational output range. For a multisine signal with fixed maximum amplitude the PAPR is a function of the phases of the individual sinusoidal components. Thus the phases can be chosen in such a way that the PAPR is minimized. No closed form solution to this problem exists, and solutions are generally found using iterative procedures. For this paper, the method described in [9] was used.

C. Impedance Recovery

To obtain the impedance of the probed magnet circuit we must estimate the amplitude and phase of both the voltage and current spectrum at the injected frequencies. The sampled current/voltage signals can be expressed similarly to (1) except now with the addition of measurement error, $\boldsymbol{\epsilon} \in \mathbb{R}^N$:

$$y_n = x_n + \epsilon_n \qquad (4)$$

To ease notation for the necessary signal processing, we convert our sampled signal, y_n, to an analytical representation through the Hilbert transform, denoted by $\tilde{\ }$. In vector notation, $\tilde{\boldsymbol{y}}$ can now be formulated as:

$$\tilde{\boldsymbol{y}} = \boldsymbol{A}\boldsymbol{\alpha} + \tilde{\boldsymbol{\epsilon}} \qquad (5)$$

where:

$$\boldsymbol{\alpha} = \left[b_1 e^{j\phi_1}, \quad b_2 e^{j\phi_2}, \quad \ldots, \quad b_K e^{j\phi_K}\right]^T, \in \mathbb{C}^K \qquad (6)$$

$$\boldsymbol{A} = \begin{bmatrix} 1 & \cdots & 1 \\ e^{j\omega_1} & \cdots & e^{j\omega_K} \\ \vdots & \ddots & \vdots \\ e^{j(N-1)\omega_1} & \cdots & e^{j(N-1)\omega_K} \end{bmatrix}, \in \mathbb{C}^{N \times K} \qquad (7)$$

To estimate the complex amplitude of the frequencies of interest we form a least squares minimization problem:

$$\underset{\hat{\boldsymbol{\alpha}} \in \mathbb{C}^K}{\text{minimize}} \quad \|\boldsymbol{A}\hat{\boldsymbol{\alpha}} - \boldsymbol{x}\|_2^2 \qquad (8)$$

One way to solve (8) is with ordinary least squares of the form [8]:

$$\hat{\boldsymbol{\alpha}} = (\boldsymbol{A}^*\boldsymbol{A})^{-1}\boldsymbol{A}^*\tilde{\boldsymbol{y}} \qquad (9)$$

where $\hat{\boldsymbol{\alpha}}$ is the estimate of $\boldsymbol{\alpha}$.

The impedance at a given frequency can be found as the ratio of the voltage and current at that frequency. For our K frequencies, the impedance can then naively be estimated as:

$$\hat{\boldsymbol{z}} = \hat{\boldsymbol{\alpha}}_v \oslash \hat{\boldsymbol{\alpha}}_i \qquad (10)$$

where:

$\hat{\boldsymbol{z}}, \hat{\boldsymbol{\alpha}}_v, \hat{\boldsymbol{\alpha}}_i \in \mathbb{C}^K$ is the estimated impedance, voltage, and current vectors of the K sinusoids.

$\oslash$ denotes element-wise division

III. MEASUREMENTS AND RESULTS

A. Experimental Setup

The performance of the system was assessed by testing it on a superconducting magnet, specifically an MBRD prototype magnet [10], using the configuration shown in Fig. 1. During the testing the magnet was connected to a thyristor based power converter (CERN designated name: RPTDA). One set of measurements was conducted with the power converter turned off, while another set was conducted with the power converter in idle mode and powering the magnet to $50\,\text{A}$. The powering test was performed with a differential voltage quench protection system attached and configured with a detection threshold and a validation time of $100\,\text{mV}$ and $10\,\text{ms}$, respectively. This system did not trip during testing indicating the non-intrusiveness of the method.

For standard electrical integrity measurements, the impedance of a magnet is measured without a power converter connected. This allows the magnet to be probed across its powering terminals. However, this is not practical when the power converter is connected, as its output filter essentially develops an AC short circuit between the magnet

terminals, thus no voltage drop will be measured. Instead, we employ the probing topology shown in Fig. 1. In this topology both outermost voltage taps of the magnet are provided with identical voltage with a return path in the center tap. Voltage drop measurements can then be performed across individual coils, or as illustrated, across an aperture (two coils). We anticipate that this topology should allow the impedance of individual coils to be measured with minimum impact from the power converter impedance.

For the tests, the measurement platform was configured with a sampling rate of $400\,\mathrm{kS/s}$, enabling the collection of the 2^{19} buffer samples in $\sim 1.3\,\mathrm{s}$. The stimuli signal was designed using (2) with $f_{\min} = \frac{1\,\mathrm{kHz}}{400\,\mathrm{kHz}}$, $f_{\max} = \frac{100\,\mathrm{kHz}}{400\,\mathrm{kHz}}$, and $L = 40$. As all the initially generated frequencies were distinct, the final number of frequency components was $K = 40$.

To have a reference baseline to compare against, the magnet was also characterised using CERN's Electrical Quality Assurance (ELQA) team's impedance analyser solution [11]. Note that the reference measurements were only performed with the power converter in the off state as this impedance analyzer is not designed for measuring energized circuits.

B. System Performance

Fig. 2 illustrates the estimated impedance of the magnet aperture for both the non-powered and powered scenario when all 2^{19} available samples are used. The reference baseline measurements are also shown. First, examining the non-powered measurements, the results obtained from the developed system show good correspondence with the reference. Similarly, when considering the powered measurements, the overall shapes of the magnitude and phase response remain comparable. However, due to the added interference from the power converter, the estimated impedance is more noisy, particularly in the lower frequency range of interest. This observation aligns with the inherent characteristics of thyristor-based power converters, which are known to introduce substantial noise below $1\,\mathrm{kHz}$. Increasing the number of samples could potentially mitigate this noise issue, enhancing the fidelity of low-frequency results. Moreover, when data processing time constraints are not paramount, achieving nearly arbitrary resolution becomes feasible. This coupled with reducing the gain and filter cutoff frequency of the ADC front-end could allow the observable frequency range to be lowered if needed. Such enhancements would position the system as a viable tool for on-line electrical integrity monitoring.

However, for real-time applications, the performance of short-duration measurements must be evaluated. For this we split the powered test's voltage/current samples into smaller chunks and perform impedance estimation on these. An example of an estimate performed with only 16k samples (equivalent to $40\,\mathrm{ms}$) is shown in Fig. 2. To evaluate how the performance changes as a function of the number of samples used, we calculate the mean squared relative error of the estimated impedance of the powered magnet with respect to the reference measurement. This is shown in the box-plot in Fig. 3. The error is calculated with:

$$\mathrm{MSRE} = \frac{1}{N} \sum_{i=1}^{N} \left\| \frac{z_i - \hat{z}_i}{z_i} \right\|_2^2 \tag{11}$$

where z and $\hat{z}$ is the reference and estimated impedance respectively.

It should be noted that with the enlargement of the window size, the number of chunks diminishes, consequently reducing the data available to derive statistical insights. As the window size decreases, both the error and the variance of the error increase. This observation is in line with estimation theory [8], and consequently it may prove difficult to identify rapidly evolving changes in the impedance profile that may occur, namely during a quench. Thus to enable more detailed quench analysis further improvements to the platform and testing conditions are required. This could for example be obtained by boosting signal power, decreasing the number of frequencies simultaneously probed, investigate the use of different stimuli signal with superior crest factor, improve the algorithm for impedance estimation, reducing peripheral noise contributions, or tailoring the front end to the specific magnet probed. Such improvements would further position the system as a vital tool in enabling novel research into the electrical characteristics of quenching magnets and quench detection techniques.
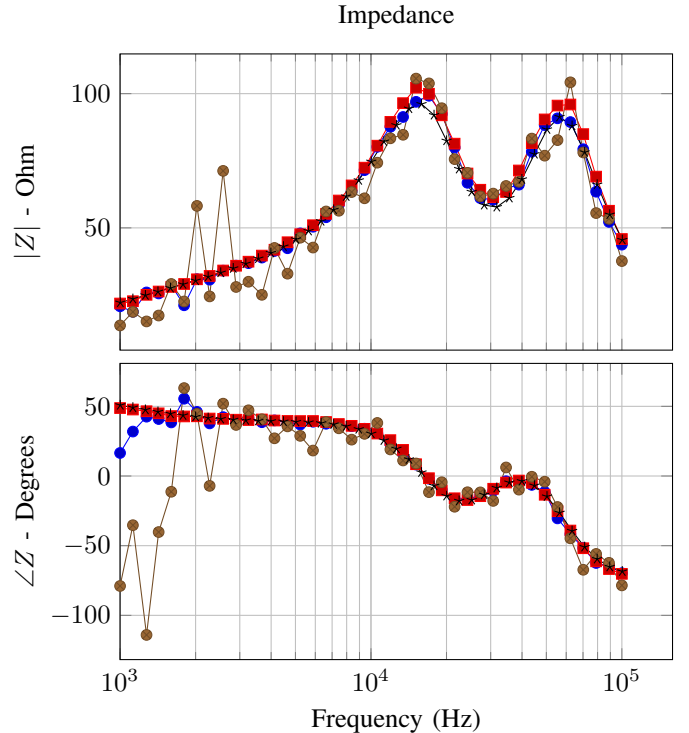

Fig. 2.   Impedance estimate based on 2^{19} samples: powered (—●—), not powered (—■—), powered - 16k samples (—●—), reference (—✳—).

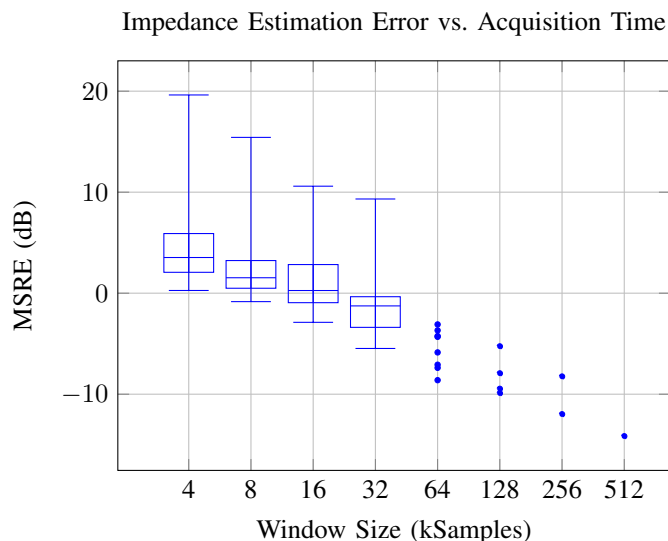## Impedance Estimation Error vs. Acquisition Time

Fig. 3. Mean squared relative error of the estimated impedance of the magnet (while powered to 50 A) with respect to the reference measurement as a function of window size.

IV. CONCLUSIONS

In this paper, we introduced a method that effectively and safely measures the impedance of a powered magnet circuit using a platform to inject low amplitude voltage stimuli into a device. Preliminary results suggest a potential for performing diagnostics of superconducting magnet circuits in real-time during their operation. Upcoming measurement initiatives aim to assess magnets energized at higher current levels to further validate the method over magnet's full operational spectrum. Additionally, the system's ability to measure short-duration impedance provides the means to monitor quenching magnets, paving the way for research into innovative quench detection methodologies. However, to realize the full extent of this capability further refinements of the short-duration impedance estimation quality is needed. This may be achieved either through algorithmic improvements, by boosting signal power, or by tailoring the platform's hardware parameters to a specific magnet target.

ACKNOWLEDGEMENT

REFERENCES

[1] A. Kotarba, P. Jurkiewicz, J. Ludwin, M. Talach, R. Mompo, M. Bednarek, and A. Board, "Automatic measurement system for electrical verification of the LHC superconducting circuits," in *IPAC*, San Sebastian, Spain, 2011, pp. 1756–1758. [Online]. Available: https://accelconf.web.cern.ch/IPAC2011/papers/TUPS093.PDF

[2] R. Denz, E. De Matteis, A. Siemko, and J. Steckert, "Next Generation of Quench Detection Systems for the High-Luminosity Upgrade of the LHC," *IEEE Transactions on Applied Superconductivity*, vol. 27, no. 4, pp. 10–13, 2017.

[3] J. Steckert, R. Denz, S. Mundra, T. Podzorny, J. Spasic, and D. G. Vancea, "Application of the Universal Quench Detection System to the Protection of the High-Luminosity LHC Magnets at CERN," *IEEE Transactions on Applied Superconductivity*, vol. 32, no. 6, 9 2022.

[4] T. Podzorny, A. Hollos, M. B. B. Christensen, M. A. Galilée, G. M. Garcia, J. Spasic, J. Steckert, M. M. Moya, R. Denz, T. Pridii, E. Organization, and A. Skoczen, "DATA ACQUISITION AND SUPERVISION SYSTEMS FOR THE HL-LHC QUENCH PROTECTION SYSTEM – PART I THE HARDWARE," *In Press*.

[5] M. A. Galilée, M. B. B. Christensen, G. M. Garcia, T. Podzorny, J. Spasic, J. Steckert, M. M. Moya, R. Denz, T. Pridii, E. Organization, and A. Skoczen, "Data acquisition and supervision for the HL-LHC Quench Protection System - part II the software stack," *In Press*.

[6] Y. Thurel, F. Bordy, and A. Charoy, "EMC concepts applied to the switching mode power converters supplying the superconductive magnets for the CERN LHC accelerator," *EMC Europe 2019 - 2019 International Symposium on Electromagnetic Compatibility*, pp. 796–801, 2019.

[7] A. Y. Kallel, D. Bouchaala, and O. Kanoun, "Critical implementation issues of excitation signals for embedded wearable bioimpedance spectroscopy systems with limited resources," *Measurement Science and Technology*, vol. 32, no. 8, 2021.

[8] P. Stoica, H. Li, and J. Li, "Amplitude estimation of sinusoidal signals: Survey, new results, and an application," *IEEE Transactions on Signal Processing*, vol. 48, no. 2, pp. 338–352, 2000.

[9] P. Guillaume, J. Schoukens, R. Pintelon, and I. Kollái, "Crest-Factor Minimization Using Nonlinear Chebyshev Approximation Methods," *IEEE Transactions on Instrumentation and Measurement*, vol. 40, no. 6, pp. 982–989, 1991.

[10] B. Caiffi, A. Bersani, R. R. Cereseto, P. Fabbricatore, S. Farinon, L. Fiscarelli, A. Foussat, F. Levi, F. Mangiarotti, A. Pampaloni, E. Todesco, S. F. Troitino, and G. Willering, "The development of the superconducting dipoles D2 for the high luminosity upgrade of LHC," *IEEE Transactions on Applied Superconductivity*, vol. 31, no. 5, 2021.

[11] J. Ludwin and P. Jurkiewicz, "Upgrade of the Automatic Measurement System for the Electrical Verification of the LHC Superconducting Circuits," *IEEE Transactions on Applied Superconductivity*, vol. 26, no. 3, pp. 1–3, 2016.